Preparation, Molecular Structure and Morphological Studies of DBSA Doped (M-Toluidine-Co-2-Ethylaniline) Copolymer Composites for flexible Sensor Applications in Agricultural Field

P S Vijayanand [1]*, A Mahudeswaran [2], J Vivekanandan [3], S Ashokan [4]

[1] *Department of chemistry, Bannari Amman Institute of Technology, Sathyamangalam, Erode, India.* vijayanandps@bitsathy.ac.in

[2, 3, 4] *Department of Physics, Bannari Amman Institute of Technology, Sathyamangalam, Erode, India*

Abstract: A new series of dodecyl benzene sulphonic acid(DBSA) doped copolymer was synthesized using two different monomers m-toluidine and 2-ethylaniline with silver nanoparticles. The synthesized copolymer nanocomposite is soluble in Dimethylformamide (DMF), Tetrahydrofuran (THF), Dimethyl sulfoxide (DMSO), and N-Methylpyrrolidone (NMP). The synthesized polymer is analysed by various characterisation techniques. The absorption peaks around 316 and 598 nm confirm the presence of π – π* transition and n – π* transition. The increase in the ethyl aniline ratio in the feed induced blue shift in the absorption peak. FTIR spectra confirms the presence of benzenoid and quinoid ring. The XRD pattern indicates the amorphous pattern of the polymer. SEM image revealed a large number of smooth surfaced particles agglomerate together. Ordered spherical sized growth of the particles with layered architectures, Nano sized tubular or nanotube growth along with porous structures was observed in the SEM image. The electroactive study of the composite confirms the semiconducting nature 1.04×10^{-6} to 2.86×10^{-8} S/cm, which can be used as basic materials for the manufacturing electric and electronic components in sensor field. The application of this electroactive materials are under taken for moisture sensor studies in the future for precision agriculture.

Keywords: Conjugated copolymer, DBSA, silver nanoparticles, optoelectronics.

1. INTRODUCTION

Nowadays, conducting polymers, such as polyaniline (PANI), polypyrrole (PPy), poly(3,4-ethylenedioxythiophene) (PEDOT), and their derivatives have attracted immerse attention in the development of flexible gas sensors owing to their easy synthesis, low operation temperature, excellent electrical conductivity, facial functionalization and flexibility. Among them, PANI has showed encouraging NH3 sensing behaviors and appeared to be the most extensively investigated candidate for room-temperature NH3 sensitive materialsConjugated polymers gain much interest in the industrial importance due to their characteristic optical, electrical properties and in turn used for manufacturing components in modern electronic devices. The polyaniline nanocomposite exhibited excellent response towards change in pH against different environmental conditions, namely standard buffer solutions with pH ranging from 2 to 10, Red and Bentonite soils, wherein the pH varied with water (soil moisture contents). The composite films based on electroactive polymers acts as a prominent material in sensor for the determination of soil pH variation in soil, water which is most essential for precision agriculture. They also find potential applications in the energy storage, sensors, coatings, optoelectronic devices, rechargeable batteries [1-2]. Precision agriculture (PA) is a farming management concept based on observing, measuring and responding to inter- and intra-field variability in crops. Precision farming is also sometimes referred to as satellite based agriculture and site-specific crop management. Hence, Precision agriculture have become one of the essential requirements in farming management system for sustainable development. In recent years, various new technologies have been developed to improve the harvest production, crop quality and the food quality. These include satellite imaging, gamma attenuation, ground penetration radar (GPR), geophysical sensors to estimate soil properties, irrigation system and laboratory analysis for soil quality [3-4]. In polyaniline macromolecule, the presence of π-conjugated system in the polymer chain results in delocalization of

electrons leading to the electrical conducting property of the material. These conjugated polymeric materials can be easily synthesized at low cost with good environmental stability [5-6]. The properties of the conjugated polymers can be enhanced by adding different type of dopants, synthesizing conjugated copolymers having different functional groups and polymer nanocomposites using metal nanoparticles [7-12].

Incorporation of metal nanoparticles in the conjugated polymer will also enhance optical and electrical properties [13-15]. Therefore, hybrid polymer composite is a combination of an organic polymer and an inorganic conducting material like carbon nanotubes, graphene and the metal nanoparticles such as silver, gold, cadmium sulphide, cadmium selenide, titanium oxide, iron oxide, zinc oxide. These nanomaterials possess unique electronic and optical properties which are different from the bulk state. Xue et, al reported that the conductivity of the conjugated polymer was found to vary linearly with increasing the iron nanoparticle in the content [16]. Stejskal et al studiedthe enhanced electrical conductivity in polyaniline with silver nanoparticles [17]. Gupta et al reported the polyaniline silver nanocomposites were found to possess superior electrical characteristic with crystalline nature and stability. The incorporation of silver nanoparticles in organic matrix decreases the band gap and as a consequently the electrical conductivity also found to increase when compared with the pure polyaniline [18]. Due to importance of the electroactive nature of material we have reported the facile synthesis, properties of poly(m-toluidne-co-2-ethylaniline) copolymer in nanoscaled dimension. Mostly the structure of the nanoscaled materials is decided by the structure of micelle core. Hence the role of DBSA can act as a structure directing agent for the growth of polymer materials in different shapes. we have tried to obtain different nanoscaled morphology using soft template in-situ polymerisation. There are plenty of application of this materials used in electronic devices like the manufacture of wireless sensor networks (WSN), including in the agriculture, military, sports, medical, and industry [19-22].

2. SYNTHESIS OF THE COPOLYMER COMPOSITES (3:3)

0.326 g (0.01 M) of DBSA was dissolved in 80 mL of pure deionised water. 0.05 M (0.5358 g) monomer toluidine and 0.05 M (0.6059 g) of 2-ethylaniline were added and stirred well. Aqueous solution of Hydrochloric acid (HCl) with 1 mL (0.03 g) of nanosilver colloidal solution is slowly injected along the walls of conical flask. At last the water soluble free radical catalyst (2.28 g) of ammonium persulfate (APS) is introduced into the reactant solution. The temperature setting ranged from 0 to 5 degrees Celsius.The resulting green precipitate was filtered, cleaned, and dried. Similar procedures were used for the 3:2 and 3:1 ratios of copolymer are prepared respectively. Figure 1 illustrates the synthesis scheme of copolymer system poly(meta - toluidine poly-co-2-ethylaniline) poly (m-tol-co-2-EA).

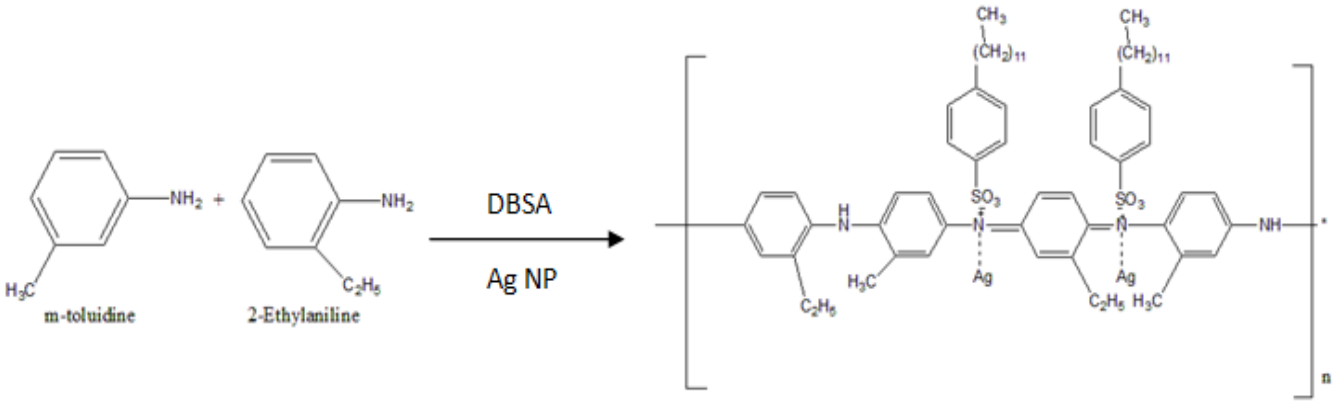

Figure 1. Reaction scheme for copolymer synthesis

2.1 Instrumentation technique

ELICO SL-218 double beam spectroscopy was employed to record the UV-Vis spectra of diluted sample in the range of 200 to 900 nm. FT-IR spectra of nanocomposites were measured by SHIMADZU 8400S in the region of 400 - 4000 cm^{-1} using KBr pellets. Scanning electron microscopy (HR-SEM) HITACHI-SU6600L instrument operating at 25 kV was used to examine the surface morphology. The phase identification of the fine powdered sample was performed by Philips X'Pert Pro X-Ray diffractometer with Nickel filtered CuKá radiation (λ=1.5402 Å) with the operation of 40 kV. The analysis was performed in the from 5 to 80° at a speed of 2°/min. 2θ diffraction angle. The room temperature

conductivity measurement of nanocomposites was measured by a standard four probe method. The samples were palletized to a diameter of 1.5 cm and a thickness of 0.4 mm using a vacuum press at 12 MPa for 5 min.

3. RESULTS AND DISCUSSION

3.1 UV-Visible spectra:

Figure 2 shows the UV-Visible spectra of poly (m-tol-co-2-EA) copolymer and the characteristic peak values are shown in the Table 1. The spectra show absorption peak at 313 nm to 319 nm, which is attributed to the π – π* transition and other peak from 581 nm to 598 nm is ascribed to n – π* transition[23]. It is observed that when monomer ratio increases, the benzenoid ring transition shifts to the lower wavelength and this blue shift. These transitions result from extended conjugation of π electron orbits, electron delocalization responsible for higher conductivity.

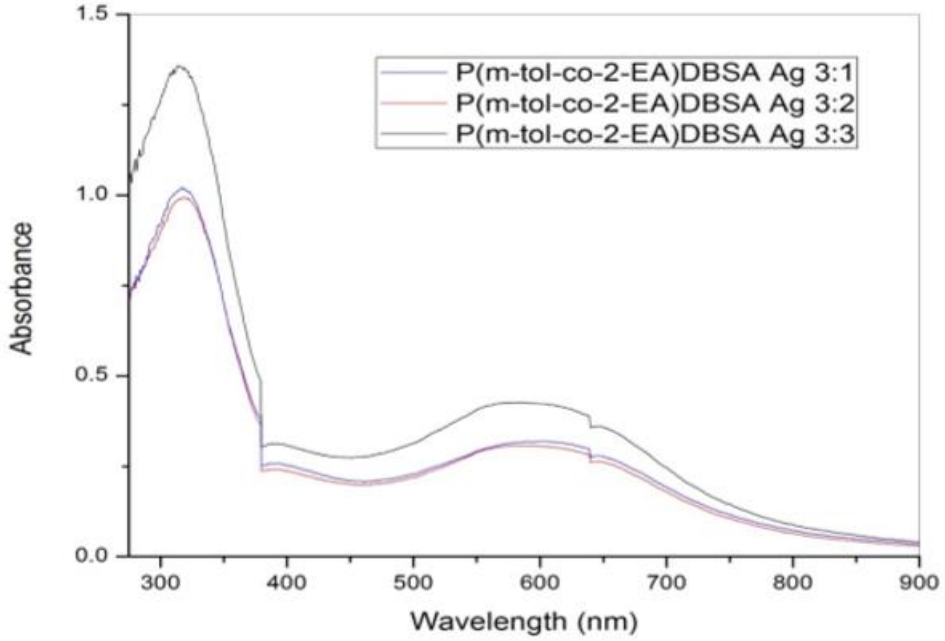

Figure 2.UV-Visible spectra of poly (m-tol-co-2-EA) DBSA Ag composites with different comonomer concentration (3:1, 3:2, 3:3)

Table 1. UV-Visible spectral values of copolymer composites

Electronic Transitions	Wavelength (nm)		
	Poly(m-tol-co-2-EA)DBSA-Ag		
	3:1	3:2	3:3
π – π* benzenoid ring transition	316	319	313
n - π* quinoid ring transition	598	590	581

3.2 FTIR spectra

Figure 3 displays the FTIR spectrum for the silver-dispersed DBSA-doped poly(m-tol-co-2-EA) copolymer composites. The peak at 3263 cm^{-1}attributed to N-H stretching vibration and it is shifted to the higher wave number. The C-H aromatic and C-H alkyl stretching values are observed at 2968 and 2873 cm^{-1}, respectively. The intense band at 1589 and 1496 cm^{-1} are attributed to CH stretching of the quinoid rings and benzenoid rings respectively. These bands confirm the formation of conjugated units in the polymer chain. The sharp peak at 1296 cm^{-1} confirms the presence of C-N stretching vibration. The C-H stretching and C-H out plane of bending of the copolymer is confirmed with the peak values at 1155 and 823 cm^{-1}, respectively [24].

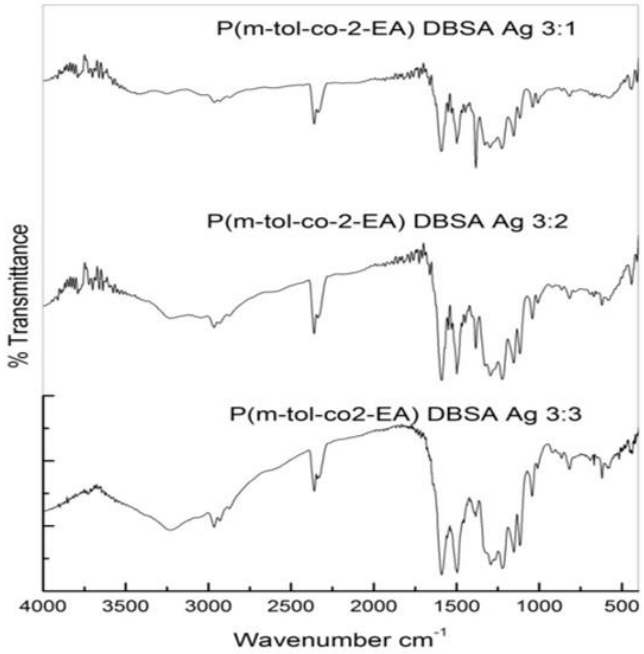

Figure 3. FTIR spectra of poly (m-tol-co-2-EA) DBSA Ag composites with different comonomer concentration (3:1, 3:2, 3:3)

3.3 XRD Studies

The XRD spectral analysis of silver dispersed poly(m-tol-co-2-EA) copolymer composites for various monomer, comonomer ratio is shown in the figure 4. The significant peak around 2θ=20° and 25°, which is connected to periodicity both perpendicular and parallel to the polymer backbone, respectively [25]. The broad peak is representing the amorphous characteristic nature of polymer. The polymer is more amorphous due to the plasticizing effect of the comonomer concentration caused from the side chainethyl substituent group in the benzene ring.

The presence of silverNanoparticles in the copolymer are confirmed with JCPDS file no. (03-0931) peaks at 38° and 44°.However, the increase of comonomer concentration in the copolymer feed constantly reduces the broadening of the amorphous peak.

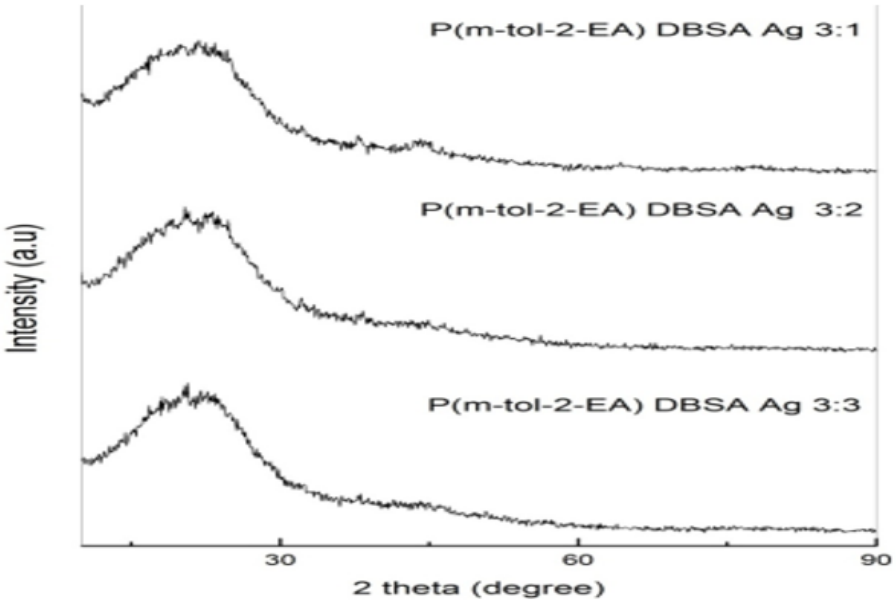

Figure 4. XRD pattern of poly (m-tol-co-2-EA) DBSA Ag composites with different comonomer concentration (3:1, 3:2, 3:3)

3.4Surface morphology

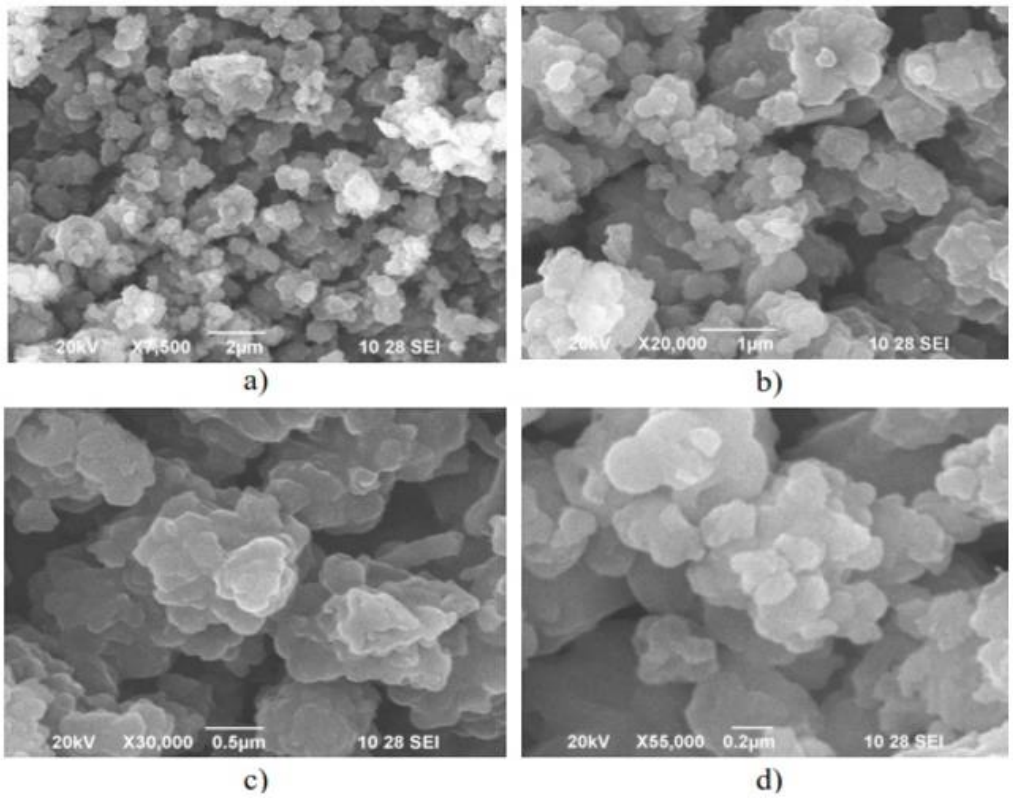

Figure.5 Surface analysis of poly (m-tol-co-2-EA) DBSA Ag comonomer composite concentration (3:3) with different magnification

Figure 5 (a, b, c & d) shows the surfactant doped Ag embedded poly (m-tol-co-2-EA) copolymer nanocomposites. The nanoparticles are agglomerated and also evenly dispersed of mixed ordered arrangement pattern. Higher magnification shows that the particle size from 100 to 200 nm. In the continuous phase, the nucleates arbitrarily grouped together to form the supramolecular structure. The initially the granule grows from the aggregated nucleus and thereby growth of polymer chains occurs by propagation from the centre, the growing polymer chain may be deposited vertically or in horizontal fashion to have a pillaring of layered granular appearance, with the smooth immersion of silver nanoparticles into it. The fused granular morphology of small spherical structures is noticed in the clusters and these particles orient or curled with themselves to have twisted form. In between there occurs a hollow structure between the different layered structure which clearly evidence the polymerisation have taken place in only in the soft template molecules. The particles show well defined boundaries, inter granular spaces between them and at some places these particles are interconnected to each other [26]. It is also observed from the image 5c, there is a formation of tubular structure reveals the controlled growth of the polymer chain within the micelle nano reactor in one particular orientation.

3.5 Electrical properties

The electrical conductivity value of nanocomposite is given in the table 2. It ranges from 3.75 to 5.06 × 10^{-8} S/cm. When comparing to the pure copolymer, decreased conductivity of the copolymer has been observed. This may be due to the more disorder manner of the copolymer chain and decrease in the crystallinity. The electrical conductivity value of the silver dispersed DBSA doped copolymer is found to be higher for 3:1 ratio than other ratios. The hopping process may take place for the increased conductivity. The steric hindrance in the copolymer may reduce the electron delocalization from the π orbital and decrease in the conjugation of the copolymer [27]. Based upon the electrical conductivity studies the prepared polymeric materials can be used fundamentally for the fabrication of flexible type humidity sensor or soil PH sensor as a real time application. This is due to the elastic nature of the polymer film which may be due to key properties of the polymer film membrane form can cause swelling by water vapor adsorption capacity, porosity, electrical conductivity while interacting with gas or liquids. The functioning of the electroactive

materials with water molecules as follows. At higher humidity environment it shows lower resistance character (consequently higher conductivity). The dopant molecules, the water molecules are weakly attached to the polymer by weak van der Waals forces of attraction. The water molecules adsorbed in the copolymer chain act as a source of proton for better electronic charge carrier.

Table 2. Electrical conductivity of poly (m-tol-co-2-EA) nanocomposites

Copolymer	Conductivity (S/cm)
Poly(An-co-2-EA) DBSA Ag 3:1	1.04×10^{-6}
Poly(An-co-2-EA) DBSA Ag 3:2	2.96×10^{-8}
Poly(An-co-2-EA) DBSA Ag 3:3	2.54×10^{-8}

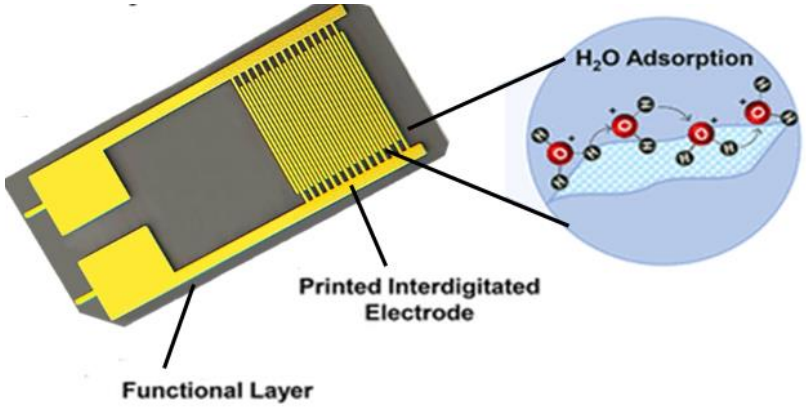

Figure 6. Schematic diagram of real time application in humidity sensor

4. CONCLUSION

The chemical oxidative polymerization process has been utilized for the preparation of new electrical poly(m-tol-co-2-EA) composites, and the chemical molecular structure of the polymers were analysed by different characterisation techniques. The FTIR spectrum clearly confirms the presence of benzenoid and quinoid responsible for electron transport. The XRD spectrum confirms the copolymer's amorphous nature. SEM images revealed the nanostructured particles with smooth morphology agglomerated each other. The copolymer nanocomposites can act as hole transporting layer in the optoelectronic devices since its conductivity values are within the range of semiconductors. The synthesized copolymer compound can be used as sensor nod and it cane used at various energy level. Furthermore, the life time of the sensor is expected to high. Based on the electroactive polymers we would like to fabricate low cost soil pH and humidity sensor, good sensitivity with soil pH variations, better stability, the sensor will possess potential application to measure variation in soil pH important for precision agriculture application

5. REFERENCES

[1]. G. Gibbons, Turning a Farm Art into Science-an Overview of Precision Farming, URL: (2000) www.precisionfarming.com

[2]. SheetalPatil , Hemant Ghadi , NiranjanRamgir , ArindamAdhikari , V. Ramgopal Rao Monitoring soil pH variation using Polyaniline/SU-8 composite film based conductometricmicrosensor, *Sensors and Actuators B: Chemical*, 286, 2019, 583-590

[3]. Zhang, L & Wan, M 2003,*Advanced Functional Materials*,**13**, 815-820.

[4]. Chaofang, D, Kui, X, Ting, C, Huiyan, L, Xiaogang, L 2011,*Journal of Wuhan University of Technology-Materials Science Edition*,**26**, 1068-1072.

[5]. Haba, Y, Sega, E, Narkis, M, Titelman, GI, Siegmann, A 2000, *Synthetic Metals*,**110**, 189-193.

[6]. Han, D, Chu, Y, Yang, L, Liu, Y &Lv, Z 2005*, Colloids and Surfaces A: Physiochemical and Engineering Aspects*, **259**, 179-187.

[7]. Mahudeswaran, A, Manoharan, D, Chandrasekaran, J, Vivekanandan, J ,Vijayanand, PS, 2015, *Materials Research*, **18**, 482-488

[8]. Long, Y, Chen, Z, Wang, N, Li, J & Wan, M 2004, *Physica B: Condensed Matter*, **344**,82-87.
[9]. Mohmoudian, MR, Alias, Y, Basirum, WJ &Ebadi, M 2011, *Current Applied Physics,***11**, 368-375.
[10]. Rawal, R, Chawla, S &Pundir, C.S 2011, *Analytical Biochemistry*, **419**, 196-204.
[11]. Vivekanandan, J, Mahudeswaran, A, Jeeva, A, Vijayanand, PS 2014, *Journal of Polymer Materials,***3**,463-475
[12]. Biswas, S, Dutta, B & Bhattacharya, S 2014, Applied Surface Science, **292**, 420-431.
[13]. Huang, L, Liao, W, Ling & Wen, T 2009, *Materials Chemistry and Physics*, **116**, 474-478.
[14]. Xue, W, Fang, K, Qiu, H, Li, J & Mao, W 2006, *Synthetic Metals*, **15**, 506-509.
[15]. Stejskal, J 2013*, Chemical Papers*, **67**,814-848.
[16]. Gupta, K, Jana, PC &Meikap AK 2010, *Synthetic Metals*, **160**, 1566-1573.
[17]. Huircán, J.I, Muñoz, C. Young, H. Von Dossow, L. Bustos, J. Vivallo, G. Toneatti, M. Comput. 2010, Electron. Agric. **74**, 258–264.
[18]. Morais, R. Matos, S.G. Fernandes, M.A. Valente, A.L. Soares, S.F. Ferreira, P. Reis, M. 2008, Comput. Electron. Agric., **64**, 120–132
[19]. Zou, T.; Lin, S.; Feng, Q.; Chen, Y. 2016, Sensors,**16**, 53
[20]. Haider Mahmood Jawad, RosdiadeeNordin, SadikKamelGharghan, Aqeel Mahmood Jawad and Mahamod Ismail, 2017, Sensors **17**, 1781
[21]. Kumar, D 2000,*Synthetic Metals*, **114**, 369-372.
[22]. De Souza, FG &Soares, BG 2006,*Polymer Testing*, **25**, 512-517.
[23]. Biswas, S, Dutta, B & Bhattacharya, S 2014, *Applied Surface Science*, **292**, 420-431.
[24]. Stejskal, J, Sapurina, I &Trchova, M 2010, Progress in Polymer Science, **35**, 1420-1481
[25]. Haba, Y, Segal, E, Nariks, M, Titelman, GI &Siegmann, A 1999, *Synthetic Metals*, **106**,59-56.

DOI: https://doi.org/10.15379/ijmst.v10i4.2404